nature physics

LETTERS

PUBLISHED ONLINE: 12 DECEMBER 2010 | DOI: 10.1038/NPHYS1852

Magnetically driven superconductivity in $CeCu_2Si_2$

O. Stockert[1]*, J. Arndt[1], E. Faulhaber[2,3], C. Geibel[1], H. S. Jeevan[1,4], S. Kirchner[1,5], M. Loewenhaupt[2], K. Schmalzl[6], W. Schmidt[6], Q. Si[7] and F. Steglich[1]

The origin of unconventional superconductivity, including high-temperature and heavy-fermion superconductivity, is still a matter of controversy. Spin excitations instead of phonons are thought to be responsible for the formation of Cooper pairs. Using inelastic neutron scattering, we present the first in-depth study of the magnetic excitation spectrum in momentum and energy space in the superconducting and the normal states of $CeCu_2Si_2$. A clear spin excitation gap is observed in the superconducting state. We determine a lowering of the magnetic exchange energy in the superconducting state, in an amount considerably larger than the superconducting condensation energy. Our findings identify the antiferromagnetic excitations as the main driving force for superconducting pairing in this prototypical heavy-fermion compound located near an antiferromagnetic quantum critical point.

Although conventional superconductivity (SC) is generally incompatible with magnetism, magnetic excitations seem to play an important role in the Cooper pair formation of unconventional superconductors such as the high-T_c cuprates or the low-T_c organic and heavy-fermion superconductors. Since the discovery of SC in $CeCu_2Si_2$ (ref. 1), antiferromagnetic (AF) spin excitations have been proposed as a viable mechanism for SC (refs 2–4). The discovery of SC at the boundary of AF order in $CePd_2Si_2$ (ref. 5) has pushed this notion into the framework of AF quantum criticality[6]. Unfortunately, such quantum critical points (QCPs) proximate to heavy-fermion superconductors typically arise under pressure, which makes it difficult to probe their magnetic excitation spectrum.

Here, we report a detailed study of the magnetic excitations in $CeCu_2Si_2$, which exhibits SC below $T_c \approx 0.6$ K. This prototypical heavy-fermion compound is ideally suited for our purpose, as SC here is in proximity to an AF QCP already at ambient pressure (see Fig. 1a). As shown in Fig. 1b, $CeCu_2Si_2$ crystallizes in a structure with body-centred tetragonal symmetry and is one of the best studied heavy-fermion superconductors and well characterized by low-temperature transport and thermodynamic measurements[7]. Moreover, those measurements in the field-induced normal state have already provided evidence that the QCP in this compound is of the three-dimensional (3D) spin-density-wave (SDW) type[8]. The spatial anisotropy of the spin fluctuations in superconducting $CeCu_2Si_2$ was measured at $T = 0.06$ K and at an energy transfer $\hbar\omega = 0.2$ meV and is shown in Fig. 1c. These magnetic correlations exhibit only a small anisotropy (a factor of 1.5) in the correlation lengths between the [110] and the [001] direction. Therefore, these quite isotropic spin fluctuations are in line with thermodynamic and transport measurements, exhibiting $C/T = \gamma_0 - a\sqrt{T}$ or $\rho - \rho_0 = AT^{\alpha}$, $\alpha = 1$–1.5 (refs 8,9), and strongly support a 3D quantum-critical SDW scenario[10]. We are able to identify the magnetic excitations in the normal state of paramagnetic, superconducting $CeCu_2Si_2$, around the incommensurate wave vector[11] of the SDW order nearby in the phase diagram (see Fig. 1a), and further establish the system's proximity to the AF QCP through the observation of a considerable slowing down in the spin dynamics. Going into the superconducting state, a spin gap opens out of a broadened quasielastic response that extends to much higher frequencies ($\times 10$ the superconducting gap). These data allow us to establish a saving in the AF exchange energy that is considerably larger than the superconducting condensation energy, thereby providing the first demonstration of the nearly quantum-critical AF excitations as the main driving force for unconventional SC.

Superconductivity and antiferromagnetism in $CeCu_2Si_2$

The SC in $CeCu_2Si_2$ we consider is close to the AF QCP, and is to be contrasted with a second superconducting dome appearing at high pressure that is thought to be associated with a valence instability and the concomitant fluctuations[9,12]. This AF QCP is located within the narrow homogeneity range of the '122' phase in the ternary chemical Ce–Cu–Si phase diagram of this tetragonal compound[13]. Correspondingly, we can prepare homogeneous samples (with slight Cu deficit) from the antiferromagnetically ordered side (A-type) and (with tiny Cu excess) from the paramagnetic, superconducting side of the QCP (S-type); in contrast, crystals very close to the 1:2:2 stoichiometry exhibit a ground state where SC and AF compete with each other without microscopic coexistence (A/S-type)[13]. The AF order was found to be an incommensurate SDW (ref. 11). At $T = 0.05$ K, well below $T_N \approx 0.8$ K, the A-type $CeCu_2Si_2$ exhibits an ordered magnetic moment $\mu_{ord} \approx 0.1\,\mu_B$ and an incommensurate propagation vector $\tau \approx (0.215\ 0.215\ 0.53)$. The latter can be ascribed to a nesting wave vector of the renormalized Fermi surface. However, a full microscopic description of the magnetic order remains to be addressed.

To study the superconducting state in $CeCu_2Si_2$ in detail, neutron scattering results (see Supplementary Information) on an S-type single crystal are presented in this Letter. A previous experiment was severely hampered by a large experimental background and a low signal-to-background ratio[14]. Thermodynamic measurements confirmed that this crystal is superconducting with a $T_c \approx 0.6$ K and an upper critical field $B_{c2}(T = 0) < 2$ T (see Supplementary Information). Elastic neutron scattering measurements did not feature resolution-limited magnetic Bragg peaks in S-type $CeCu_2Si_2$ in accordance with thermodynamic measurements. However, at positions where

[1]Max-Planck-Institut für Chemische Physik fester Stoffe, 01187 Dresden, Germany, [2]Institut für Festkörperphysik, Technische Universität Dresden, 01062 Dresden, Germany, [3]Gemeinsame Forschergruppe Helmholtz-Zentrum Berlin — TU Dresden, 85747 Garching, Germany, [4]I. Physikalisches Institut, Universität Göttingen, 37077 Göttingen, Germany, [5]Max-Planck-Institut für Physik komplexer Systeme, 01187 Dresden, Germany, [6]Jülich Centre for Neutron Science, Forschungszentrum Jülich, Outstation at Institut Laue–Langevin, 38042 Grenoble, France, [7]Department of Physics and Astronomy, Rice University, Houston, Texas, 77005, USA. *e-mail: stockert@cpfs.mpg.de.

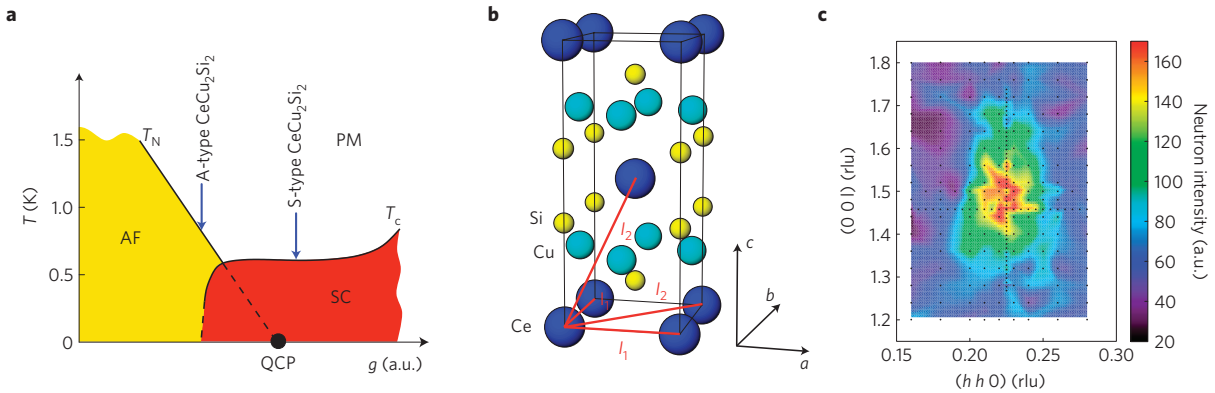

Figure 1 | Schematic phase diagram around the QCP, crystal structure and nearly isotropic spin fluctuations of $CeCu_2Si_2$. a, Schematic T–g phase diagram of $CeCu_2Si_2$ in the vicinity of the quantum critical point (QCP) where the antiferromagnetic (AF) phase vanishes as a function of the effective coupling constant g. Superconductivity (SC) is observed around the QCP and extends far into the paramagnetic (PM) regime. The composition as well as hydrostatic pressure can be used to change the coupling constant g and to tune the system to the QCP. The positions of the A-type and the S-type single crystals in the phase diagram are marked. **b**, Tetragonal crystal structure (space group: $I4/mmm$) of $CeCu_2Si_2$. The nearest- and next-nearest-neighbour interactions between the cerium atoms are labelled I_1 and I_2. It should be noted that the distances between next-nearest-neighbour Ce atoms in the basal plane and out-of-plane are almost identical. **c**, The spin fluctuations at $T = 0.06$ K and $B = 0$ and at an energy transfer $\hbar\omega = 0.2$ meV. The anisotropy factor between the [110] and the [001] directions is about 1.5. Note that the correct aspect ratio [110]* : [001]* has been taken into account although the axes are labelled in reciprocal lattice units (rlu). Black dots mark the $(\mathbf{Q}, \omega)$ positions at which data were taken.

magnetic satellite peaks are observed in A-type $CeCu_2Si_2$ (ref. 11), for example, at $\mathbf{Q}_{AF} = (0.215\ 0.215\ 1.458)$, relative to a nearby nuclear Bragg reflection $\mathbf{G}$ ($\mathbf{Q}_{AF} = \mathbf{G} \pm \tau$), the S-type crystal exhibits quite weak correlation peaks at low temperatures[14]. They are still present above T_c and disappear at $T \approx 0.8$ K, very similar to the behaviour of the SDW order in A-type $CeCu_2Si_2$ (ref. 11). Although these peaks were found to be purely elastic within the energy resolution ($\approx$57 μeV), their linewidth in $\mathbf{Q}$ space is considerably broadened, corresponding to a correlation length of 50–60 Å, comparable to the superconducting coherence length of order 100 Å (ref. 15). Thus, static magnetically ordered regions seem to exist in a fairly small part of the sample and are separated from the surrounding superconducting regions.

Spin dynamics in $CeCu_2Si_2$

We probe the magnetic response of $CeCu_2Si_2$ through extensive inelastic neutron scattering measurements around $\mathbf{Q} = \mathbf{Q}_{AF} = (0.215\ 0.215\ 1.458)$, as no appreciable magnetic intensity has been detected elsewhere in the Brillouin zone. Figure 2a shows energy scans at this $\mathbf{Q}_{AF}$ position and at a general position, $\mathbf{Q} = \mathbf{Q}_{arb} = (0.1\ 0.1\ 1.6)$, where no correlation peaks emerge, but which has the same $|\mathbf{Q}|$. Both data sets were recorded in the superconducting state at $T = 0.07$ K. At $\mathbf{Q}_{arb}$ only the incoherent elastic background contribution is seen with the instrumental resolution, and no magnetic intensity could be detected. In contrast, at $\mathbf{Q}_{AF}$ the response shows a strong inelastic signal with a long intensity tail extending beyond $\hbar\omega = 2$ meV (see inset of Fig. 2a). The missing spectral weight at low energies is an indication of a spin excitation gap in the superconducting state. The spectrum recovers the missing weight at the gap edge, thereby constituting an inelastic line. The data can be described by a quasielastic Lorentzian line with a spin excitation gap $\hbar\omega_{gap} \approx 0.2$ meV and with a density of states as for the electronic gap of a d-wave Bardeen–Cooper–Schrieffer (BCS) superconductor (solid lines in Figs 2a and 3a). $\hbar\omega_{gap} \approx 3.9 k_B T_c$ is found to be 10% smaller than the value predicted for a weak-coupling d-wave superconductor[16] and falls 20% below $2\Delta_0/k_B T_c = 5.0$, as determined by copper nuclear quadrupole resonance for $CeCu_2Si_2$ (refs 17,18). To unambiguously relate the inelastic magnetic excitation to the superconducting state, it was necessary to carry out additional measurements in the normal state.

Energy scans recorded at $\mathbf{Q}_{AF}$ in the normal state are shown in Fig. 2b. Notably, independent of how the normal state is reached, that is, above T_c at $T = 0.8$ K and $B = 0$ or above B_{c2} at $T = 0.07$ K and $B = 2$ T, the magnetic response is almost identical and seems to be quasielastic. The fits to the quasielastic magnetic response with a Lorentzian line shape give a good description of the data, as seen in Figs 2b and 3a. With increasing temperature in the normal state the magnetic response weakens in intensity and broadens considerably. Starting from $\Gamma \approx 0.11$ meV at $T = 0.07$ K the linewidth of the quasielastic response at $\mathbf{Q}_{AF}$ increases to $\Gamma \approx 0.235$ meV at $T = 1.7$ K (Fig. 3b). This considerable slowing down of the response when lowering the temperature indicates the proximity of S-type $CeCu_2Si_2$ to the AF QCP. $\Gamma(T)$ extrapolates to a finite value at $T \to 0$, as the S-type single crystal is located on the paramagnetic side of the QCP (see Fig. 1a). A related critical slowing down was observed in magnetically ordered A-type $CeCu_2Si_2$ (ref. 19).

The fact that the magnetic excitation gap disappears in the normal state, that is, above T_c, and also above B_{c2} at low temperatures, where the magnetic short-range correlations still persist, gives direct evidence that the spin gap $\hbar\omega_{gap}$ is related to the superconducting state. Its temperature variation is plotted in Fig. 3c and has been derived from fits to the data shown in Figs 2a and 3a and additional scans. As indicated by the solid line, $\hbar\omega_{gap}$ follows, within the error bars, the BCS form for the superconducting gap amplitude $2\Delta(T)$.

We now turn to the momentum dependence of the magnetic response around $\mathbf{Q}_{AF}$ in the superconducting state. Figure 4 shows $\mathbf{Q}$ scans along $(h\ h\ 1.458)$ across $\mathbf{Q}_{AF}$ recorded at different energy transfers $\hbar\omega$ and at $T = 0.06$ K. The single peak seen at $\hbar\omega \approx 0.2$ meV splits on increasing energy transfer into two peaks, which move apart from each other accompanied by a marked decrease in intensity. Fits with two peaks of Gaussian line shape (solid lines) yield a good description of the data. The peak positions for different $\hbar\omega$, shown in the inset of Fig. 4a, yield a linear dispersion relation. We conclude that the spin excitations are part of an overdamped dispersive mode. Its velocity, as read off the slope of the dispersion curve, $v_{exc} = (4.44 \pm 0.86)$ meV Å, is substantially smaller than the strongly renormalized Fermi velocity $v_F^* \approx 57$ meV Å (ref. 15) (1 meV Å = 153 m s^{-1}). This indicates a retardation of the coupling between the heavy quasiparticles and the quantum-critical spin excitations.

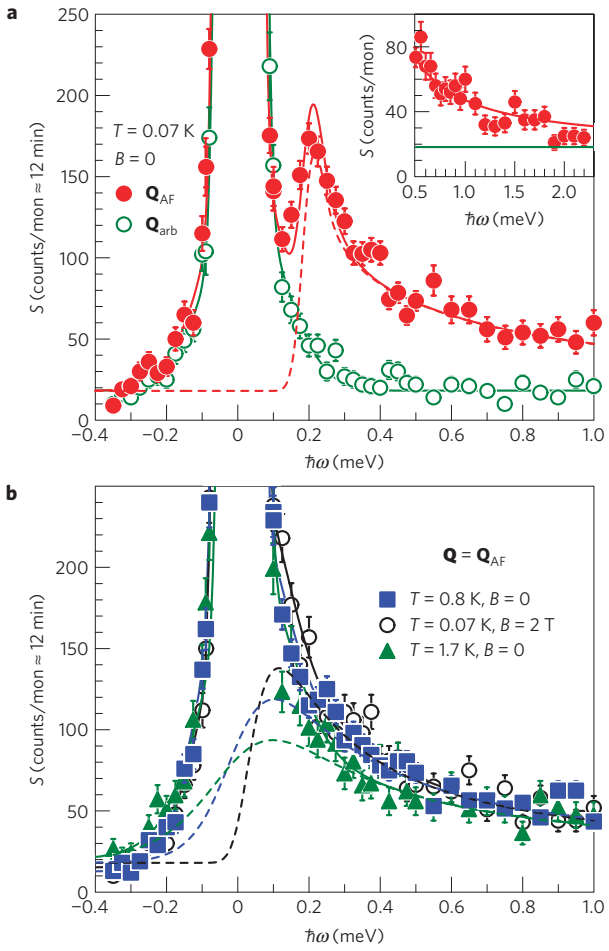

Figure 2 | Inelastic neutron scattering spectra in the normal and superconducting states of $CeCu_2Si_2$. a,**b**, Energy scans (neutron intensity $S = S_{ela} + S_{qe/ine,mag}$ versus energy transfer $\hbar\omega$) in S-type $CeCu_2Si_2$ at $\mathbf{Q} = \mathbf{Q}_{AF} = (0.215\ 0.215\ 1.458)$ in the superconducting state at $T = 0.07$ K, $B = 0$ (**a**) and in the normal state at $T = 0.8$ and 1.7 K, $B = 0$ and $T = 0.07$ K, $B = 2$ T (**b**). For comparison the magnetic response at an arbitrary, general $\mathbf{Q}$ position $\mathbf{Q} = \mathbf{Q}_{arb} = (0.1\ 0.1\ 1.6)$ at $T = 0.07$ K, $B = 0$ is also plotted in **a**. The inset in **a** shows the magnetic response at $\mathbf{Q}_{AF}$ ($T = 0.07$ K, $B = 0$) extending beyond $\hbar\omega = 2$ meV. The solid lines represent fits to the data comprising the incoherent and coherent elastic signal S_{ela} and the quasielastic/gapped inelastic magnetic response $S_{qe/ine,mag}$ (dashed lines) with Lorentzian line shape convolved with the resolution. The gapped magnetic response at $T = 0.07$ K, $B = 0$ has been modelled by a quasielastic Lorentzian line, taking into account a spin gap with a value $\hbar\omega_{gap}$ and an enhanced density of states above the gap, as for the electronic gap of a BCS superconductor. The error bars represent the statistical error.

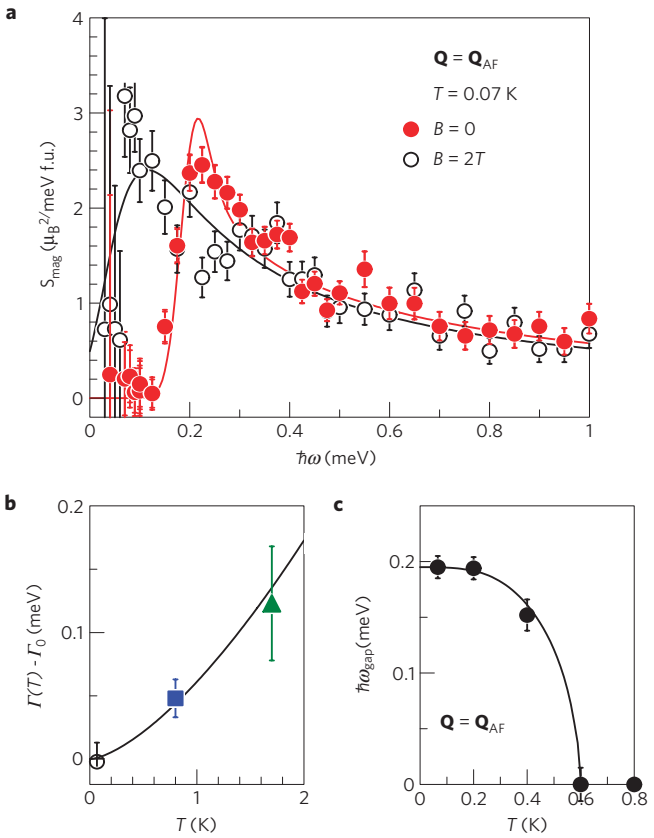

Figure 3 | Magnetic response, relaxation rate and spin gap at the AF wave vector of $CeCu_2Si_2$. a, Magnetic response $S_{qe/ine,mag}$ at $\mathbf{Q}_{AF}$ and $T = 0.07$ K in the superconducting and the normal state, that is, at $B = 0$ and $B = 2$ T, as extracted from the data shown in Fig. 2. The data have been put on an absolute intensity scale (see Supplementary Information). Below $\hbar\omega \approx 0.1$ meV (approximately 1.6 times the instrumental resolution) the errors in S_{mag} increase strongly (some data points fall even outside the plotted range), because the strong elastic scattering S_{ela} is subtracted from the total scattering to obtain S_{mag} and also because of small uncertainties in the resolution function. These uncertainties are the same for both data sets and are irrelevant, as only the difference is analysed for the estimation of the exchange energy saving. **b**, Linewidth Γ versus temperature T of the quasielastic magnetic response at $\mathbf{Q}_{AF}$ in the normal state, as yielded by fits to the data shown in Fig. 2. Plotted here is $\Gamma(T)$-Γ_0 versus T, with $\Gamma_0 = 0.112$ meV. The solid line $\Gamma(T)$-$\Gamma_0 = aT^{3/2}$ (with $a = 0.061$ meV K$^{-1.5}$) is the expected behaviour near a 3D SDW QCP. **c**, Temperature dependence of the spin excitation gap $\hbar\omega_{gap}$ at $\mathbf{Q}_{AF}$ together with the scaled d-wave BCS superconducting gap function (solid line). The error bars denote the statistical error.

Superconducting condensation and exchange energies

The observed spin excitations both below and above T_c allow us to estimate the decrease of magnetic exchange energy in the superconducting state as compared with the putative normal state. This saving of exchange energy is determined as follows[20,21]:

$$\Delta E_x \equiv E_x^{N} - E_x^{S} = \frac{1}{g^2 \mu_B{}^2} \int_0^{\infty} \frac{d(\hbar\omega)}{\pi} [n(\hbar\omega) + 1] \times \langle I(\mathbf{q})[\mathrm{Im}\chi^{N}(\mathbf{q},\omega) - \mathrm{Im}\chi^{S}(\mathbf{q},\omega)] \rangle$$

where E_x^{N} and E_x^{S} are respectively the exchange energy in the normal and superconducting states, $\langle\ \rangle$ indicates an average over the first Brillouin zone, and $\mathbf{q} = (q_x, q_y, q_z)$ denotes momentum transfer in the first Brillouin zone, that is, $\mathbf{Q} = \mathbf{G} + \mathbf{q}$. $I(\mathbf{q})$ is the exchange interaction between the localized f-moments and contains nearest (I_1) and next-nearest (I_2) neighbour terms:

$$I(\mathbf{q}) = I_1[\cos(q_x a) + \cos(q_y a)] + I_2 f_2(a, c, \mathbf{q})$$

where a and c are the lattice constants and the precise form of f_2 is given in the Supplementary Information. The inclusion of the next-nearest-neighbour terms is a consequence of the 3D nature of the spin excitations of $CeCu_2Si_2$ (see Fig. 1c). This is different from the cuprate superconductors and, for example, $CeCoIn_5$, where the observed behaviour is predominantly 2D. As described in detail in the Supplementary Information, we find a

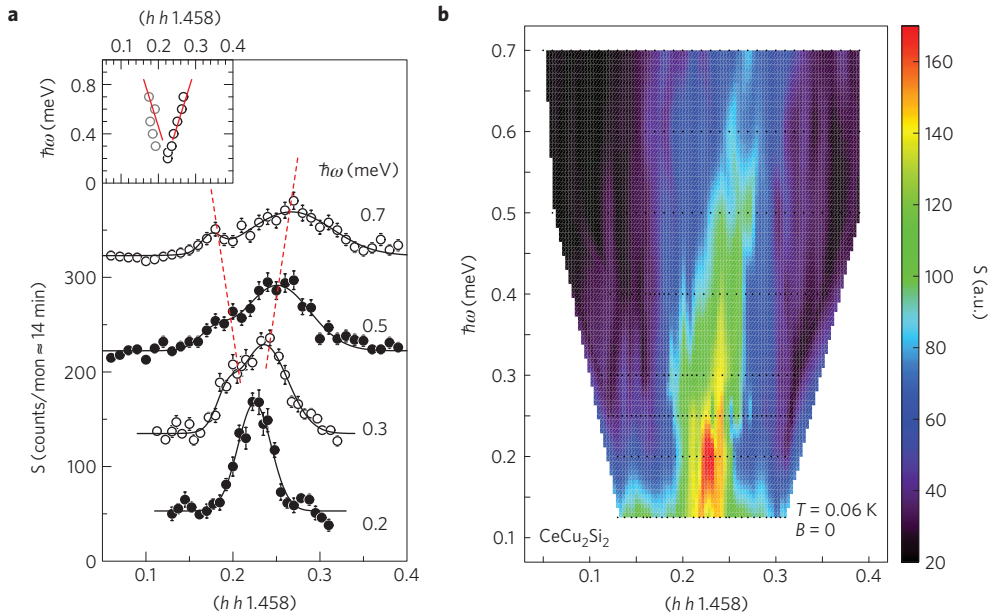

Figure 4 | Dispersion of the magnetic response in superconducting $CeCu_2Si_2$. a, Wave vector **Q** dependence of the magnetic response around $\mathbf{Q}_{AF}$ in S-type $CeCu_2Si_2$ in the superconducting state at $T = 0.06$ K for different energy transfers $\hbar\omega$. The scans are shifted by 100 counts with respect to each other. Solid lines denote fits of two peaks with Gaussian line shape to the data and dashed lines are only guides to the eye. From the linewidth at small energy transfers a dynamic correlation length $\xi \approx 25$ Å is inferred. Inset: Dispersion of the magnetic excitation around $\mathbf{Q}_{AF}$ at $T = 0.06$ K as a result of the fits to the **Q** scans. The solid line indicates a fit to the data with a linear dispersion relation, yielding a velocity $v_{exc} = (4.44 \pm 0.86)$ meV Å (for comparison spin-wave velocities in other heavy-fermion metals, UPd_2Al_3: $v = 10$–15 meV Å (ref. 36), URu_2Si_2: $v \approx 45$ meV Å; ref. 42). The error bars represent the statistical error. **b**, Colour-coded intensity plot of the data shown in **a** and additional data, clearly indicating the dispersion of the gapped spin excitation. The black dots mark the $(\mathbf{Q}, \omega)$ positions at which data were taken.

magnetic exchange energy saving of $\Delta E_x = \eta\, 4.8 \times 10^{-3}$ meV per Ce ($\eta \approx 1.25$, η being a measure of the SC volume fraction (see Supplementary Information)). This energy saving stems primarily from the spectrum at low energies below the magnetic excitation gap. This follows from the fact that the spin excitations are peaked around the wave vector $\mathbf{Q}_{AF}$ at which $I(\mathbf{q})$ is positive. Figure 5 illustrates which part of the spectrum of $\mathrm{Im}\chi(\mathbf{Q}_{AF}, \omega)$ increases/decreases ΔE_x. This energy gain must be compared with the superconducting condensation energy ΔE_C, which is the difference in internal energy between the (putative) normal and the superconducting state at $T = 0$ (refs 20,21):

$$\Delta E_C = U_N(T = 0) - U_S(T = 0)$$

Using the specific-heat data shown in Supplementary Fig. S1a, we find the condensation energy to be $\eta\, 2.27 \times 10^{-4}$ meV per Ce. Compared with the high-T_c cuprates where similar analyses have been carried out[22–24], the considerably lower energy scales in the heavy-fermion systems enable us to carry out a quantitative analysis of the data in terms of an accessible putative normal state. As noted above, extrapolating the spin excitations from above T_c is in good qualitative agreement with the excitations of the field-driven normal state at the lowest temperatures. Furthermore, the electronic specific heat of both the superconducting and normal state can be reliably determined as phonons do not contribute at such low temperatures. Despite this apparent advantage of heavy-fermion systems, ΔE_C and ΔE_x have not received much attention in the context of heavy-fermion SC. ΔE_C has been determined for $CeCoIn_5$ (ref. 25). The proximity of this compound to quantum criticality is not yet certain, as SC sets in before AF order can develop. Our study represents the first determination of the saving in both the exchange energy and the condensation energy for a superconductor near an AF QCP, as well as for any unconventional low-temperature superconductor.

Our observation that the magnetic exchange energy saving is more than one order of magnitude larger than the condensation energy implies that AF excitations are the primary driving force for SC. A comparable factor of exchange energy saving over condensation energy has recently been observed in the unconventional superconductor $YbBa_2Cu_3O_{6.6}$ (ref. 24). As described above, the temperature dependence of $\omega_{gap}(T)$ in $CeCu_2Si_2$ follows a rescaled BCS form. For a conventional BCS superconductor, where $\Theta_D \gg \omega_{gap}$, the saving in potential energy is enhanced over the condensation energy by a factor that depends logarithmically on the ratio of Debye temperature Θ_D and superconducting gap $\omega_{gap}(T = 0)$ (ref. 26). The corresponding enhancement factor over the condensation energy in $CeCu_2Si_2$, where the Kondo temperature $T_K \approx 15$ K replaces the Debye temperature Θ_D, turns out to be two. The fact that the observed magnetic energy saving is more than a factor 20 larger than the condensation energy indicates a large loss in kinetic energy. A natural origin for this loss lies in the Kondo effect, as the kinetic energy of the quasiparticles appears through the Kondo-interaction term. As superconducting pairing in $CeCu_2Si_2$ occurs in the spin-singlet channel, the opening of the superconducting gap therefore weakens the Kondo-singlet formation and, by extension, reduces the spectral weight of the Kondo resonance (see Supplementary Information).

Comparison with other unconventional superconductors

Our understanding of the magnetic exchange energy saving in the heavy-fermion superconductor $CeCu_2Si_2$ near its AF QCP naturally leads us to ask whether the effect is universal. SC-induced enhancement of the spin-fluctuation spectrum in some frequency range has also been observed in high-T_c cuprates such as $YBa_2Cu_3O_{7-\delta}$ (ref. 27), iron pnictides such as K- or Co-doped $BaFe_2As_2$ (refs 28,29) or $FeTe_{1-x}Se_x$ (refs 30,31), as well as two other heavy-fermion compounds, UPd_2Al_3 (refs 32,33) and $CeCoIn_5$ (ref. 25). However, there are some striking differences

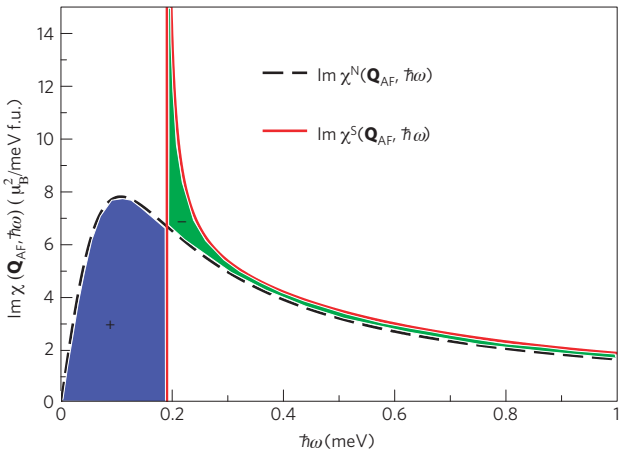

Figure 5 | Schematic plot of the imaginary part of the dynamic spin susceptibility Im$\chi(\mathbf{Q}_{AF},\omega)$ in the normal and superconducting states. The dynamic correlation function $S(\mathbf{Q}_{AF},\omega)$ of Fig. 3a is related to Im$\chi(\mathbf{Q}_{AF},\omega)$ through the fluctuation-dissipation theorem after deconvolving the data with the instrument's energy resolution function. The blue area (marked with a '+') leads to an increase in ΔE_x, whereas the green area (marked with a '−') leads to a decrease in ΔE_x. The fact that the opening of the gap contributes to the saving of exchange energy is a consequence of $I(\mathbf{Q}_{AF}) > 0$ at the wave vector $\mathbf{Q}_{AF}$, where Im$\chi^{N/S}(\mathbf{Q},\omega)$ is peaked.

between the spectrum observed in $CeCu_2Si_2$ and those seen in the other superconductors. In contrast to $CeCu_2Si_2$, where SC and long-range AF order exclude each other, SC in UPd_2Al_3 occurs inside the antiferromagnetically ordered part of its magnetic phase diagram, which is far away from any QCP (ref. 34). Whether a QCP underlies SC in the cuprates, the iron pnictides or $CeCoIn_5$, is yet to be established. The normal-state magnetic response of S-type $CeCu_2Si_2$ at $\mathbf{Q}_{AF}$ slows down considerably when lowering the temperature, indicating its proximity to a QCP, and exhibits pronounced dispersion. $CeCu_2Si_2$ represents, therefore, the only system in which we can unambiguously establish the link between AF quantum criticality and unconventional SC, even though the effect may well prove to be broadly relevant. In comparison with other heavy-fermion superconductors, the inelastic spin response in $CeCu_2Si_2$ is broad in energy and extends beyond ten times the gap value, whereas in $CeCoIn_5$ a rather sharp, resolution-limited spin resonance is found[25]. Furthermore, unlike $CeCoIn_5$, the temperature dependencies of the spin excitation gap in $CeCu_2Si_2$ and UPd_2Al_3 (ref. 35) do follow the expected BCS form. In comparison with $CeCu_2Si_2$, UPd_2Al_3 also exhibits a dispersive spin excitation starting at the low-energy inelastic line (related to the edge of the spin gap[33]) with a slightly higher in-plane mode velocity[36]. However, the situation in the cuprate superconductors is more complex, with an hour-glass-like dispersion of the resonance mode[37–39].

Experimentally, the most prominent difference between $CeCu_2Si_2$ and other unconventional superconductors is the $\mathbf{Q}$ position of the spin excitation gap, which is observed in all reported unconventional superconductors at or close to simple commensurate positions with half-integer indices. For example, in UPd_2Al_3 and $CeCoIn_5$it occurs at commensurate positions, $\mathbf{Q} = (0\ 0\ 1/2)$ and $(1/2\ 1/2\ 1/2)$ respectively[25,36]. In contrast, in S-type $CeCu_2Si_2$ the gapped spin excitations are restricted to the vicinity of the ordering wave vector of the system, $\tau \approx (0.215\ 0.215\ 0.53)$, which is incommensurate, far away from a simple commensurate value. As a result, the opening of a spin gap becomes the main source of exchange energy saving. By extension, an additional excitonic resonance in $\chi^S(\mathbf{Q},\omega)$ due to the superconducting state[40] would reduce the energy saving. This is a striking difference between $CeCu_2Si_2$ on the one hand, and $CeCoIn_5$(ref. 25) and high-T_c cuprate superconductors[23] on the other.

Our inelastic neutron scattering experiments in $CeCu_2Si_2$ reveal spin excitations associated with the AF (3D-SDW) QCP. These spin excitations are overdamped, dispersive and gapped in the superconducting state. Our quantitative estimate of both the change in magnetic exchange energy and the superconducting condensation energy identifies the AF excitations as a main driving force for SC. At present, AF QCPs are being explored in a variety of strongly correlated electron systems, including the new Fe pnictide superconductors. $Ba(Fe_{1-x}Co_x)_2As_2$ (ref. 41), for instance, exhibits a T–x phase diagram very similar to the T–p phase diagram of $CePd_2Si_2$, raising the prospect that AF quantum-critical excitations also drive the superconducting pairing in these new high-T_c superconductors.

Methods

High-resolution inelastic neutron scattering experiments were carried out on the cold-neutron triple-axis spectrometer IN12 at the high-flux reactor of the Institut Laue–Langevin in Grenoble/France. A vertical focusing graphite (002) monochromator and a doubly focused (vertical and horizontal) graphite (002) analyser were used. The horizontal collimation was provided by the neutron guide in front of the monochromator and 60′ before the sample, whereas no collimation was provided in the scattered beam. A liquid-nitrogen-cooled Be filter was placed in the incident neutron beam to reduce higher-order contamination. The measurements were carried out with a fixed final wave vector $k_f = 1.15$ Å^{-1}, which corresponds to a final neutron energy $E_f = 2.74$ meV and yields a high energy resolution $\Delta E \approx 57$ μeV full-width at half-maximum. All experiments were carried out on an S-type $CeCu_2Si_2$ single crystal ($m \approx 2$ g). The crystal was mounted with the $[1\bar{1}0]$ axis vertical on a copper pin attached to the mixing chamber of a dilution refrigerator. The set-up results in a [110]–[001] scattering plane. Data were taken at temperatures between $T = 0.06$ and 1.7 K and in magnetic fields up to $B = 2.5$ T applied along the vertical $[1\bar{1}0]$ axis. The inelastic neutron scattering measurements were converted to units of μ_B^2/(meV f.u.) by normalizing the intensities to the incoherent scattering of the sample.

Received 16 November 2009; accepted 18 October 2010; published online 12 December 2010

References

1. Steglich, F. *et al.* Superconductivity in the presence of strong Pauli paramagnetism: $CeCu_2Si_2$. *Phys. Rev. Lett.* **43,** 1892–1896 (1979).
2. Miyake, K., Schmitt-Rink, S. & Varma, C. M. Spin-fluctuation-mediated even-parity pairing in heavy-fermion superconductors. *Phys. Rev. B* **34,** 6554–6556 (1986).
3. Scalapino, D. J., Loh, E. & Hirsch, J. E. d-wave pairing near a spin-density-wave instability. *Phys. Rev. B* **34,** 8190–8192 (1986).
4. Monthoux, P., Pines, D. & Lonzarich, G. G. Superconductivity without phonons. *Nature* **450,** 1177–1183 (2007).
5. Mathur, N. D. *et al.* Magnetically mediated superconductivity in heavy fermion compounds. *Nature* **394,** 39–43 (1998).
6. Gegenwart, P., Si, Q. & Steglich, F. Quantum criticality in heavy-fermion metals. *Nature Phys.* **4,** 186–197 (2008).
7. Steglich, F. *et al. More is Different—Fifty Years of Condensed Matter Physics* 191–210 (Princeton Univ. Press, 2001).
8. Gegenwart, P. *et al.* Breakup of heavy fermions on the brink of 'Phase *A*' in $CeCu_2Si_2$. *Phys. Rev. Lett.* **81,** 1501–1504 (1998).
9. Yuan, H. Q. *et al.* Observation of two distinct superconducting phases in $CeCu_2Si_2$. *Science* **302,** 2104–2107 (2003).
10. Rosch, A. Interplay of disorder and spin fluctuations in the resistivity near a quantum critical point. *Phys. Rev. Lett.* **82,** 4280–4283 (1999).
11. Stockert, O. *et al.* Nature of the A phase in $CeCu_2Si_2$. *Phys. Rev. Lett.* **92,** 136401 (2004).
12. Holmes, A. T., Jaccard, D. & Miyake, K. Signatures of valence fluctuations in $CeCu_2Si_2$ under high pressure. *Phys. Rev. B* **69,** 024508 (2004).
13. Steglich, F. *et al.* New observations concerning magnetism and superconductivity in heavy-fermion metals. *Physica B* **223–224,** 1–8 (1996).
14. Stockert, O. *et al.* Magnetism and superconductivity in the heavy-fermion compound $CeCu_2Si_2$ studied by neutron scattering. *Physica B* **403,** 973–976 (2008).
15. Rauchschwalbe, U. *et al.* Critical fields of the 'heavy-fermion' superconductor $CeCu_2Si_2$. *Phys. Rev. Lett.* **49,** 1448–1451 (1982).
16. Ohkawa, F. Cooper pairs of $d_{x^2-y^2}$-symmetry in simple square lattices. *J. Phys. Soc. Jpn* **56,** 2267–2270 (1987).
17. Ishida, K. *et al.* Evolution from magnetism to unconventional superconductivity in a series of $Ce_xCu_2Si_2$ compounds probed by Cu NQR. *Phys. Rev. Lett.* **82,** 5353–5356 (1999).

18. Fujiwara, K. *et al.* High pressure NQR measurement in $CeCu_2Si_2$ up to sudden disappearance of superconductivity. *J. Phys. Soc. Jpn* **77,** 123711 (2008).
19. Stockert, O. *et al.* Peculiarities of the antiferromagnetism in $CeCu_2Si_2$. *J. Phys.: Conf. Ser.* **51,** 211–218 (2006).
20. Scalapino, D. J. & White, S. R. Superconducting condensation energy and an antiferromagnetic exchange-based pairing mechanism. *Phys. Rev. B* **58,** 8222–8224 (1998).
21. Leggett, A. Where is the energy saved in cuprate superconductivity? *J. Phys. Chem. Solids* **59,** 1729–1732 (1998).
22. Demler, E. & Zhang, S-C. Quantitative test of a microscopic mechanism of high-temperature superconductivity. *Nature* **396,** 733–735 (1998).
23. Woo, H. *et al.* Magnetic energy change available to superconducting condensation in optimally doped $YBa_2Cu_3O_{6.95}$. *Nature Phys.* **2,** 600–604 (2006).
24. Dahm, T. *et al.* Strength of the spin-fluctuation-mediated pairing interaction in a high-temperature superconductor. *Nature Phys.* **5,** 217–221 (2009).
25. Stock, C., Broholm, C., Hudis, J., Kang, H. J. & Petrovic, C. Spin resonance in the d-wave superconductor $CeCoIn_5$. *Phys. Rev. Lett.* **100,** 087001 (2008).
26. Haslinger, R. & Chubukov, A. V. Condensation energy in strongly coupled superconductors. *Phys. Rev. B* **68,** 214508 (2003).
27. Sidis, Y. *et al.* Magnetic resonant excitations in high-T_c superconductors. *Phys. Status Solidi B* **241,** 1204–1210 (2004).
28. Christianson, A. D. *et al.* Unconventional superconductivity in $Ba_{0.6}K_{0.4}Fe_2As_2$ from inelastic neutron scattering. *Nature* **456,** 930–932 (2008).
29. Inosov, D. S. *et al.* Normal-state spin dynamics and temperature-dependent spin-resonance energy in optimally doped $BaFe_{1.85}Co_{0.15}As_2$. *Nature Phys.* **6,** 178–181 (2010).
30. Qiu, Y. *et al.* Spin gap and resonance at the nesting wave vector in superconducting $FeSe_{0.4}Te_{0.6}$. *Phys. Rev. Lett.* **103,** 067008 (2009).
31. Lumsden, M. D. *et al.* Evolution of spin excitations into the superconducting state in $FeTe_{1-x}Se_x$. *Nature Phys.* **6,** 182–186 (2010).
32. Bernhoeft, N. *et al.* Enhancement of magnetic fluctuations on passing below T_c in the heavy fermion superconductor UPd_2Al_3. *Phys. Rev. Lett.* **81,** 4244–4247 (1998).
33. Sato, N. K. *et al.* Strong coupling between local moments and superconducting 'heavy' electrons in UPd_2Al_3. *Nature* **410,** 340–343 (2001).
34. Link, P., Jaccard, D., Geibel, C., Wassilew, C. & Steglich, F. The heavy-fermion superconductor UPd_2Al_3 at very high pressure. *J. Phys. Condens. Matter* **7,** 373–378 (1995).
35. Bernhoeft, N. *et al.* Magnetic fluctuations above and below T_c in the heavy fermion superconductor UPd_2Al_3. *Physica B* **259–261,** 614–620 (1999).
36. Hiess, A. *et al.* Magnetization dynamics in the normal and superconducting phases of UPd_2Al_3: I. Surveys in reciprocal space using neutron inelastic scattering. *J. Phys. Condens. Matter* **18,** R437–R451 (2006).
37. Pailhès, S. *et al.* Resonant magnetic excitations at high energy in superconducting $YBa_2Cu_3O_{6.85}$. *Phys. Rev. Lett.* **93,** 167001 (2004).
38. Hayden, S. M., Mook, H. A., Dai, P., Perring, T. G. & Dogan, F. The structure of the high-energy spin excitations in a high-transition-temperature superconductor. *Nature* **429,** 531–534 (2004).
39. Tranquada, J. M. *et al.* Quantum magnetic excitations from stripes in copper oxide superconductors. *Nature* **429,** 534–538 (2004).
40. Eremin, I., Zwicknagl, G., Thalmeier, P. & Fulde, P. Feedback spin resonance in superconducting $CeCu_2Si_2$ and $CeCoIn_5$. *Phys. Rev. Lett.* **101,** 187001 (2008).
41. Chu, J-H., Analytis, J. G., Kucharczyk, C. & Fisher, I. R. Determination of the phase diagram of the electron-doped superconductor $Ba(Fe_{1-x}Co_x)_2As_2$. *Phys. Rev. B* **79,** 014506 (2009).
42. Wiebe, C. R. *et al.* Gapped itinerant spin excitations account for missing entropy in the hidden-order state of URu_2Si_2. *Nature Phys.* **3,** 96–99 (2007).

Acknowledgements

We greatly acknowledge helpful discussions with A. Chubukov, P. Coleman, T. Dahm, I. Eremin, B. Fåk, A. Hiess, D. Scalapino and P. Thalmeier. This work was supported by the Deutsche Forschungsgemeinschaft through Forschergruppe 960 'Quantum phase transitions', as well as by the NSF Grant No. DMR-1006985 and the Robert A. Welch Foundation Grant No. C-1411.

Author contributions

H.S.J. and C.G. synthesised the sample. O.S., J.A., E.F., M.L., K.S. and W.S. carried out the measurements. O.S., J.A. and S.K. analysed the data. S.K. and Q.S. carried out theoretical calculations. O.S., S.K., Q.S. and F.S. wrote the manuscript. O.S., S.K., Q.S. and F.S. planned and managed the project.

Additional information

The authors declare no competing financial interests. Supplementary information accompanies this paper on www.nature.com/naturephysics. Reprints and permissions information is available online at http://npg.nature.com/reprintsandpermissions. Correspondence and requests for materials should be addressed to O.S.